Atmospheric
Chemistry
and Physics

Supplement of

Estimation of OH in urban plumes using TROPOMI-inferred NO$_2$ / CO

Srijana Lama et al.

Correspondence to: Srijana Lama (s.lama@vu.nl, sreejanalama@gmail.com)

Text S1. Chemical transformation of NOx to HNO₃

The passive tracer transport method in WRF is used for this study extended with the first order loss of NO_x as explained here. The chemical transformation of NOx to HNO_3 is performed in the following steps:

Step 1: The NOx and CO emission at the surface level, CAMS derived OH concentration and CAMS derived NOx/NO_2 derived from surface to model level 30 is introduced in WRF chem using the emission input files.

Step 2: The WRF-Chem module for passive tracer has been modified to account for the removal of NOx by OH. First, we calculate the IUPAC second order rate constant for the reaction between NO_2 and OH, using pressure and temperature for each vertical level. Secondly, the OH effect on NOx is calculated for each vertical level using the equations below:

$$\mathbf{fact} = \frac{\mathbf{NOx}}{\mathbf{NO_2}}$$

$$\mathbf{XNO_{x(emis,OH)}} = \left(\frac{\mathbf{K}}{\mathbf{fact}}\right) * \mathbf{CAMS\ OH} * \mathbf{dtstep} * \mathbf{XNO_{x\ emis}}$$

Here, K is the IUPAC second order rate constant, $XNO_{x\ emis}$ is the tracer linearly related to EDGAR NOx emission and $\mathbf{XNO_{x(emis,OH)}}$ is the tracer accounting the effect of OH.

Text S2. Derivation of EMG method

$$\tau_{NO2} = \frac{x_o}{U}$$
x_o is the downwind decay length [km] obtained from EMG method and U [m/s] is the boundary layer averaged wind speed for the box 300kmx100km. The unit of lifetime is hr .
$$\tau_{NO2} = \frac{1}{K_{NO2\ OH}[OH]}$$

Converting the hour into second

$$\tau_{NO2}*60.0*60.0 = \frac{1}{K_{NO2\ OH}[OH]}$$
$$OH \qquad = \frac{1}{\tau_{NO2}*60.0*60.0* K_{NO2\ OH}}$$

$K_{NO2\ OH}$ is the IUPAC second order rate constant [$s^{-1}molecules^{-1}cm^3$] and OH [$moleculescm^{-3}$] is the hydroxyl radical concentration over Riyadh at time TROPOMI overpasses.

Text S3. Conversion of NO₂ emission in molecule cm⁻¹ into mole second⁻¹

$$E_{NO2} * U$$
Converting the ms^{-1} into cm s^{-1} and molecules into moles
$$\frac{E_{NO2}*U*100}{6.023e^{23}}$$

E_NO₂ is the NO_2 emission [molecule cm^{-1}] obtained from EMG method. U [m s^{-1}] is the wind speed.

Text S4. Least square optimization

We have model M to simulate data d_{mod} with the given model parameter x
$$d_{mod} = M(x)$$

For the non-linear case, the model search the most probable solution of x at the minimum of cost function (J)
.

$$J_{(x)} = \frac{1}{2} \cdot \left[\left(d_{obs} - M(x)\right)^T R^{-1} \left(d_{obs} - M(x)\right) + (x - x_0)^T B^{-1}(x - x_0) \right]$$

$$R = \begin{bmatrix} \sigma_{d1}^2 & . & cov(d3,d1) \\ . & \sigma_{d2}^2 & . \\ cov(d1,d3) & . & \sigma_{d3}^2 \end{bmatrix} \quad B = \begin{bmatrix} \sigma_{dx1}^2 & . & cov(x3,x1) \\ . & \sigma_{dx2}^2 & . \\ cov(x1,x3) & . & \sigma_{x3}^2 \end{bmatrix}$$

The cost function has two terms, the first measures the distance between the observations(d_{obs}) and the model (M), the second measures the distance between the parameter(x) solution and its first guess (x_0). R and B are the covariance matrices for d_{obs} and x, showing their uncertainty.

Text S5 Iterative scaling factor optimization

Step 1: Scaling factors f_{OH1}, f_{emis1} and f_{Bg1} (for OH, emissions and background levels) are derived from least squares optimization of WRF using a priori settings to TROPOMI.

Step 2: WRF is run with optimized inputs from Step 1 to derive WRF Ratio $_{1st\,iter}$, $XNO_{2\,1st\,iter}$ and $XCO_{WRF,\,1st\,iter}$.

Step 3: f_{OH2}, f_{emis2} and f_{Bg2} are derived as in Step 1 using the results from Step 2.

Step 4: Step 2 is repeated for f_{OH2}, f_{emis2} and f_{Bg2} to derive WRF Ratio$_{opt}$, $XNO_{2\,WRF,opt}$ and $XCO_{WRF,\,opt}$.

Step 5: Final optimized scaling factor are derived by multiplying the scaling factor from the 1st and 2nd iteration.

Text S6. Uncertainty estimation on OH concentration, NO_x and CO emission using least square method and EMG method

For the error calculation, the relative change in the OH concentration, NO_x and CO emission with alteration in the width of box, downwind length of box , wind speed and NO_2 bias correction is estimated. The width of the box is changed from 100km to 90 km and 110km. Downwind length of box is changed from 200km to 190km and 210km. For the effect of wind speed, we used WRF wind data and compare the results with the CAMS wind data. To estimate the error from NO_2 bias ,the difference between the S5P-PAL reprocessed NO_2 (see https://sentinels.copernicus.eu/documents/247904/0/Sentinel-5P-Nitrogen-Dioxide-Level-2-Product-Readme-File/3dc74cec-c5aa-40cf-b296-59a0f2140aaf) and bias corrected NO_2 is used. Sha et al.,(2021) compared the TROPOMI derived XCO to the 28 different TCCON ground based station and concluded that average difference between TCCON and TROPOMI is in the range of 9.1 ± 3.3 % . Such difference is used for the calculation of uncertainty.
Our method accounts only for NOx removal by OH, neglecting the contribution of other NOx removal pathways to the lifetime of NOx. A sensitivity test using WRF-chem with VOC-NOx chemistry shows that this introduces an our OH estimates of ~5 % in summer and ~20 % in winter. Furthermore, to check if the size of the error matches the expected contribution of other NOx removal pathways the Chemistry Land-surface Atmosphere Soil Slab (CLASS) (van Stratum et al., 2012) model has been used. CLASS provides Ox-NOx-VOC-HOx photochemistry scheme with 28 different chemical reaction including the loss of NO_x via N_2O_5 to HNO_3. We run the CLASS model for a summer and winter day representative of Riyadh. During the summer mid-day, NO_x loss is dominated by OH (93.4 %) in CLASS. The heterogeneous N_2O_5 loss accounts for 6.6 % (see Figure S27), in close agreement with the full chemistry WRF test. During the winter mid-day, the N_2O_5 loss increases to 21.4 % and NO_2+OH accounts for 78.6 % of the total NO_x loss (see Fig S27), which is larger than the mismatch in the full chemistry test, but within its uncertainty.

The estimated uncertainties for the scaling factors f_{emis}, f_{OH} and f_{Bg} are derived by summing the contribution of wind speed, length and width of the box ,NO_2 bias correction and other sources of NOx loss in quadrature as presented in Tables S1 and S2. For summer and winter, the uncertainties of the optimized OH concentrations is <17 % and <29 % respectively. For NOx and CO emissions, the uncertainty is < 29 % in summer and winter.

Text S7. X^2 calculation

$$X^2 = \frac{\sum_{i=1}^{n} \frac{(Observed_i - expected_i)^2}{\sigma^2_i}}{N}$$

Where the observed data are the TROPOMI retrievals and expected data are the results of the WRF optimization, σ is the prior uncertainty and N is the number of observations.

Table S1. Estimated uncertainties in f_{emis}, f_{OH} and f_{Bg} obtained by ratio optimization of XNO_2 and XCO for summer and winter over Riyadh. The description of each component contributing to the uncertainty in f_{emis}, f_{OH} and f_{Bg} is provided in Text S6.

	Uncertainty Summer (%)			Uncertainty Winter (%)		
	OH	Emission ratio	Bg ratio	OH	Emission ratio	Bg ratio
Width of the box (A)	4.8	2.5	1.0	8.2	16.0	4.1
Downwind length (B)	4.5	3.2	1.7	4.0	12.0	3.0
Wind speed (C)	8.4	8.4	8.4	4.1	4.1	4.1
NO2 Bias Correction (D)	6.3	5.4	2.0	13.0	53.0	13.2
CO Bias (E)	8.8	12.8	3.0	9.2	9.0	8.7
NOx loss by N_2O_5 +H_2O (F)	6.7	x	x	21.1	x	x
Total Uncertainty $\left(\sqrt{\begin{pmatrix} \mathbf{A^2 + B^2 + C^2 + D^2 + E^2} \\ +F^2 + G^2 \end{pmatrix}}\right)$ **(%)**	16.6	16.7	9.35	28.26	57.5	17.1

Table S2. Same as Table S1 but the estimated uncertainties in f_{emis}, f_{OH} and f_{Bg} obtained by component wise optimization of XNO_2 and XCO. The description of each component contributing to the uncertainty in f_{emis}, f_{OH} and f_{Bg} is provided in Text S6.

	Uncertainty Summer (%)					Uncertainty Winter (%)				
	OH	NOx Emission	NOx Bg	CO Emission	CO Bg	OH	NOx Emission	NOx Bg	CO emission	CO Bg
Width of the box (A)	5.8	10.0	9.8	9.1	8.7	8.1	6.5	4.1	9.4	4.5
Downwind length (B)	4.5	4.5	1.5	0.9	0.2	2.9	3.4	3	1.4	0.5
Wind speed (C)	8.4	8.4	8.4	8.4	8.4	4.1	4.1	4.1	4.1	4.1
NO_2 Bias Correction (D)	5.0	10.0	2.0	x	x	11.0	13.5	11.0	X	x
CO Bias (E)	x	x	x	14.2	11.2	x	x	x	18.1	20.0

NOx loss by N_2O_5 +H_2O (F)	6.7	10.6	x	9.5	x	21.1	23.1	x	10.5	x
Total Uncertainty (%)	13.9	20.07	13.1	21.1	16.48	25.63	27.9	12.8	23.3	20.9

Table S3. Same as Table S1 but the estimated uncertainties in OH and NOx emission obtained by EMG method. The description of each component contributing to the uncertainty in NOx emission and OH is provided in Text S6.

	Uncertainty Summer (%)		Uncertainty Winter (%)	
	OH	Emission	OH	Emission
Width of the box (A)	4.0	7.5	4.0	10.0
Downwind length (B)	2.0	2.5	2.0	10.0
Wind speed (C)	8.4	8.4	4.1	4.1
NO2 Bias (D)	5.0	11.3	12.0	16.6
Total Uncertainty (%) $(\sqrt{(A^2 + B^2 + C^2 + D^2)}$	10.8	16.14	13.4	22.18

Table S4. Overview of optimized emission ratio, OH and background ratio using ratio and component wise optimization. Th ratio of NOx emission/CO emission is the emission ratio. The ratio of NO_2 background/ CO background is the background ratio.

Variables	Summer			Winter		
	Prior	Ratio optimization	Component optimization	Prior	Ratio optimization	Component optimization
Emission ratio (NOx emission /CO emission)	0.79 (8.2/10.34)	2.01±0.33	0.55±0.091 (11.6/21.09)	0.93 (9.4/10.1)	1.46±0.8	0.36±0.18 (7.8/21.6)
OH (10^7, molecules/cm^3)	1.3	1.7± 0.3	1.66±0.23	0.86	1.3±0.38	1.28±0.32
Background ratio (XNO_{2Bg}/XCO_{Bg})	0.002 (0.22/92.13)	6.8e-04± 6.12e-05	5.9e-04± 7.6e-05 (0.053/88.41)	0.0016 (0.15/92.58)	5.3e-04 ±1.5e-04	5.4e-04±1.5e-04 (0.049/90.54)

Table S5. Comparison of EDGAR CO emission 2012, 2018 with the Optimized CO emission over Riyadh at the time TROPOMI overpasses. Emission presented below includes diurnal, weekly and monthly emission factor.

	2012 (EDGAR v4.3.2)		2012 (EDGAR v5.0)		2018 (EDGAR v5.0)		OPTIMIZED EMISSION for (EDGAR v4.3)	
	Summer	Winter	Summer	Winter	Summer	Winter	Summer	Winter
CO emission (kg/s)	10.34	10.1	11.86	11.45	16.4	15.8	21.09	21.6

Table S6. Overview of WRF optimized OH and NOx emissions for Riyadh using NOx background with and without the loss by OH.

Parameters	Summer			Winter		
	Prior	Optimized using Bg without OH loss	Optimized using Bg with OH loss	Prior	Optimized using Bg without OH loss	Optimized using Bg with OH loss
NOx emission (kg/s)	8.2	11.6 ± 2.4	11.1	9.4	7.9 ± 1.8	8.03
OH (1e7, molecules/cm3)	1.3	1.7 ± 0.2	1.67	0.86	1.3 ± 0.14	1.22
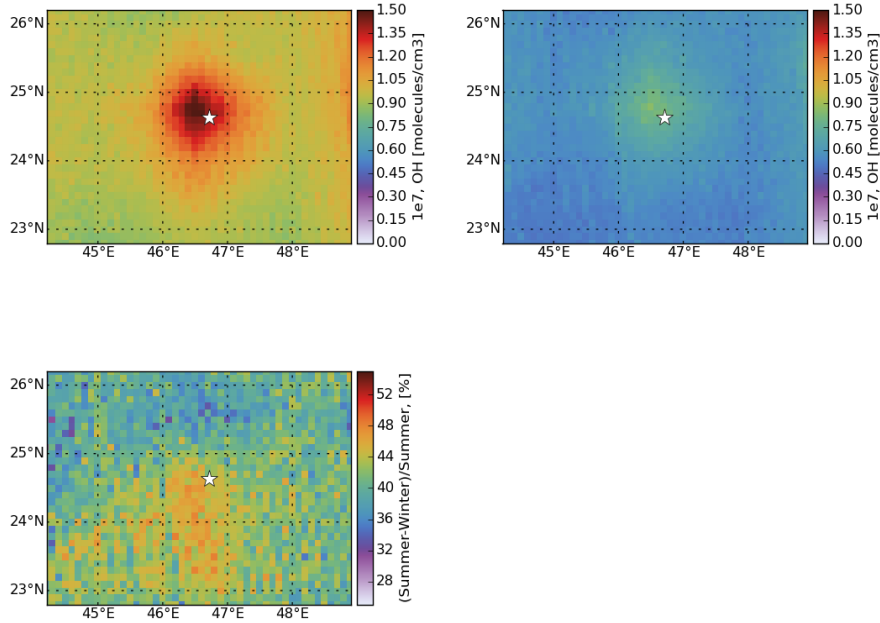
Figure S1. Boundary layer averaged CAMS OH concentration a) Summer, b) Winter and c) Relative difference over Riyadh at the time TROPOMI overpasses.
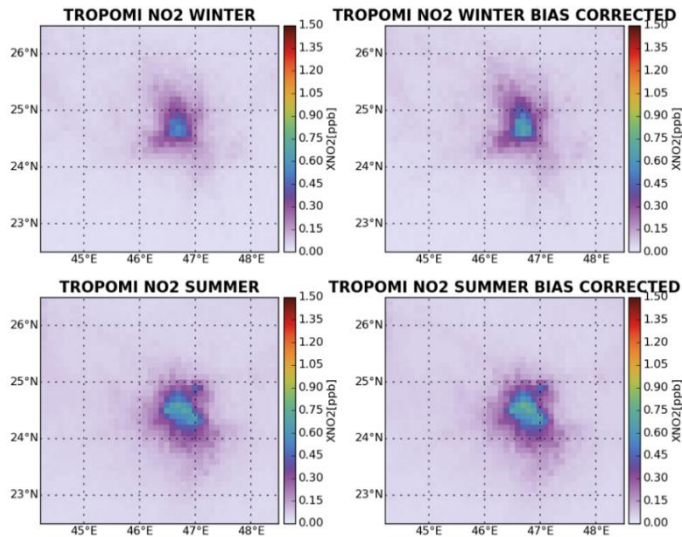
Figure S2. TROPOMI derived XNO2 before and after bias correction using AMF recalculation for summer (bottom) and winter (top) over Riyadh.

6
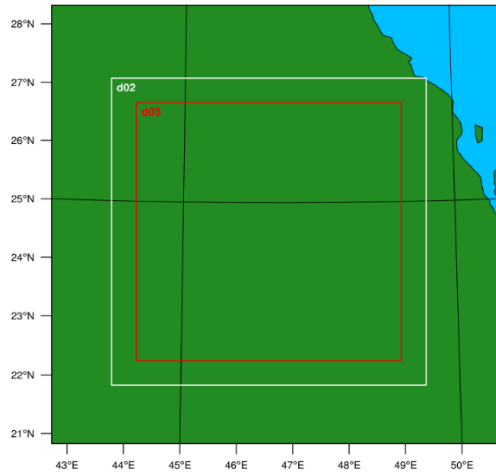
Figure S3. WRF domains d01, d02 and d03 with the spatial resolutions of 27km, 9km and 3 km over Riyadh
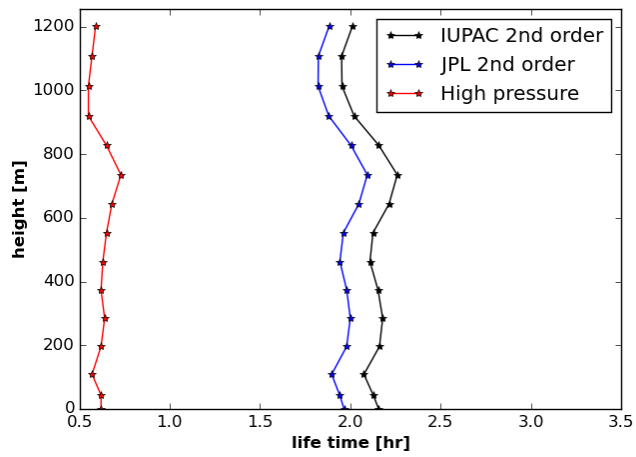
Figure S4. Lifetime profile for high pressure rate constant, JPL 2nd order and IUPAC 2nd order rate constant at the center of Riyadh
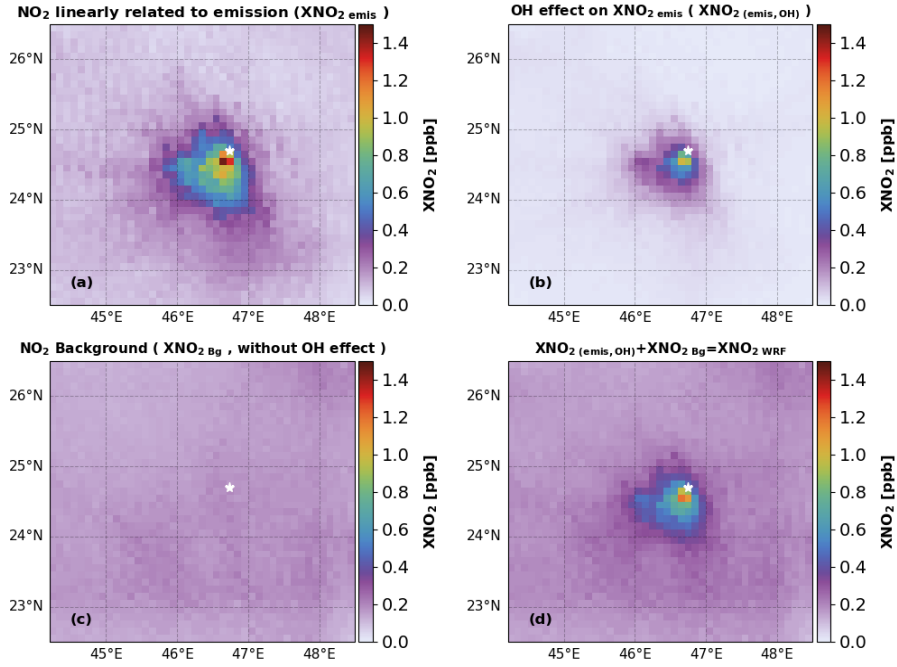
Figure S5. WRF simulated NO$_2$ a) linearly related to emission $(XNO_{2,emis})$ b) OH effect on $XNO_{2,emis}$ ($XNO_{2,(emis,OH)}$) c) NO$_2$ background based on CAMS $(XNO_{2\,Bg})$ and d) sum of $XNO_{2,(emis,OH)}$ and $XNO_{2\,Bg}$ to derive $XNO_{2\,WRF}$ over Riyadh averaged from June to October, 2018.
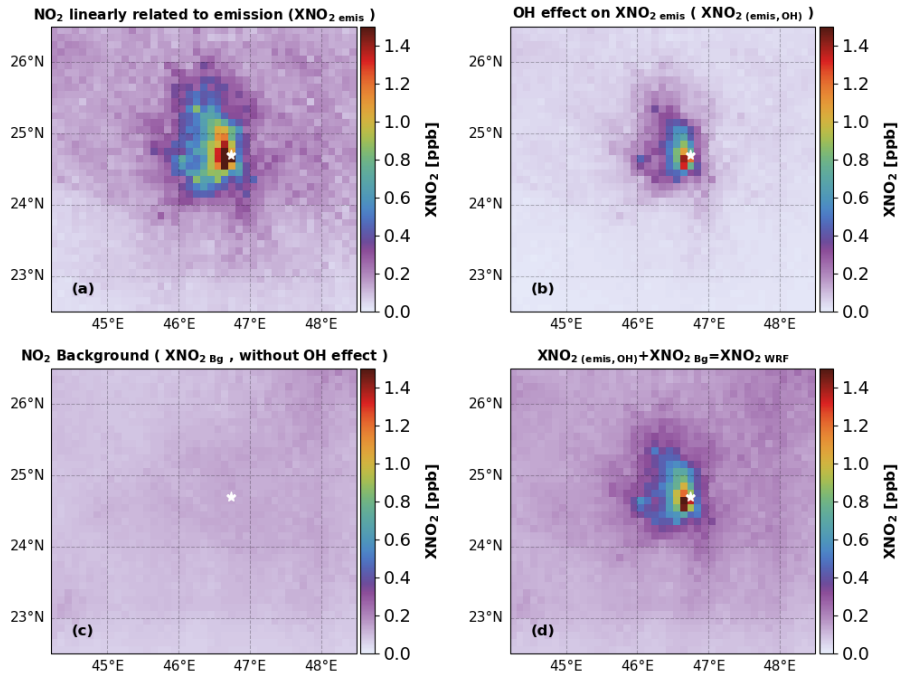
Figure S6. Same as Fig. S5 but for winter (November, 2018 to March, 2019)
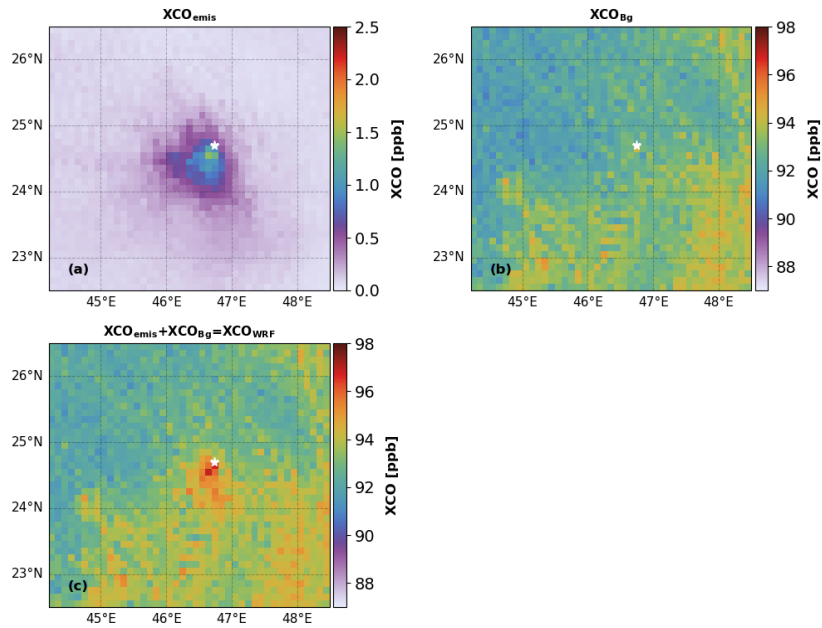
Figure S7. WRF simulated CO a) linearly related to emission (XCO_{emis}), b) background based on CAMS (XCO_{Bg}) and c) sum of XCO_{emis} and XCO_{Bg} to derive XCO_{WRF} over Riyadh averaged from June to October, 2018.
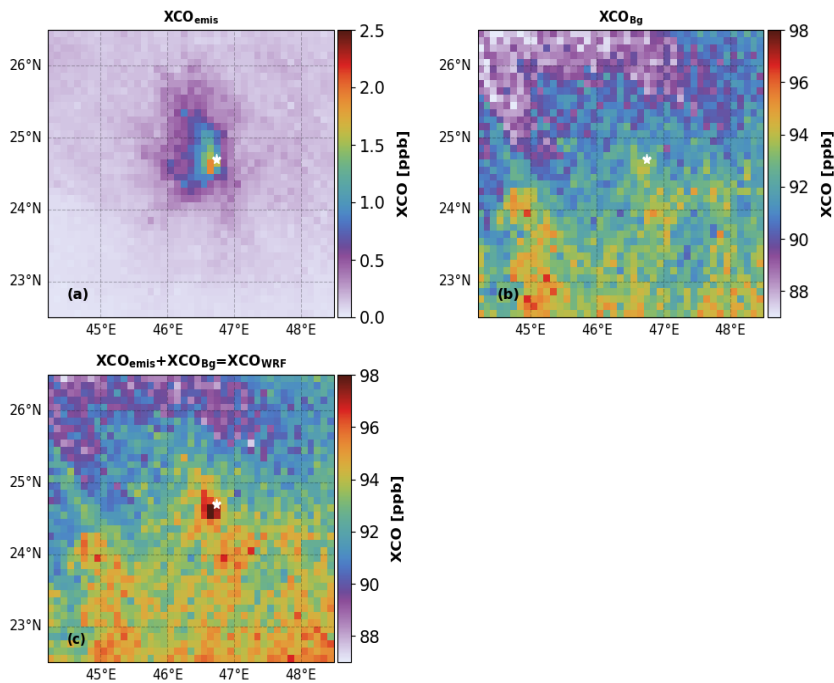
Figure S8. Same as Fig. S7 but for winter (November, 2018 to March, 2019)
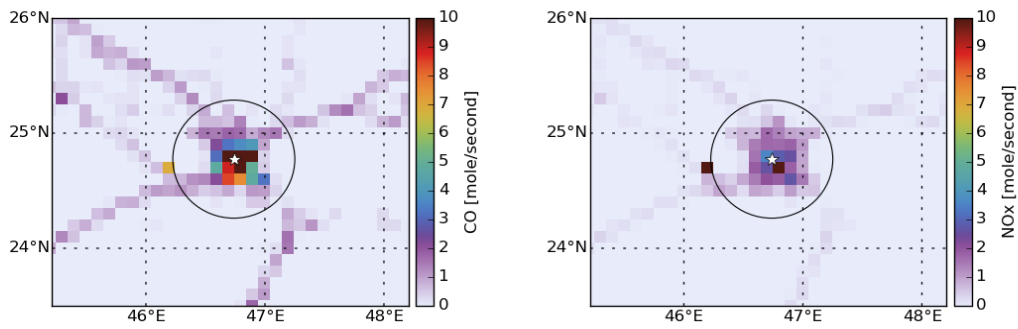
Figure S9. EDGAR 2012 CO (left) and NOx (right) emission over Riyadh. The white star represents the center of Riyadh.
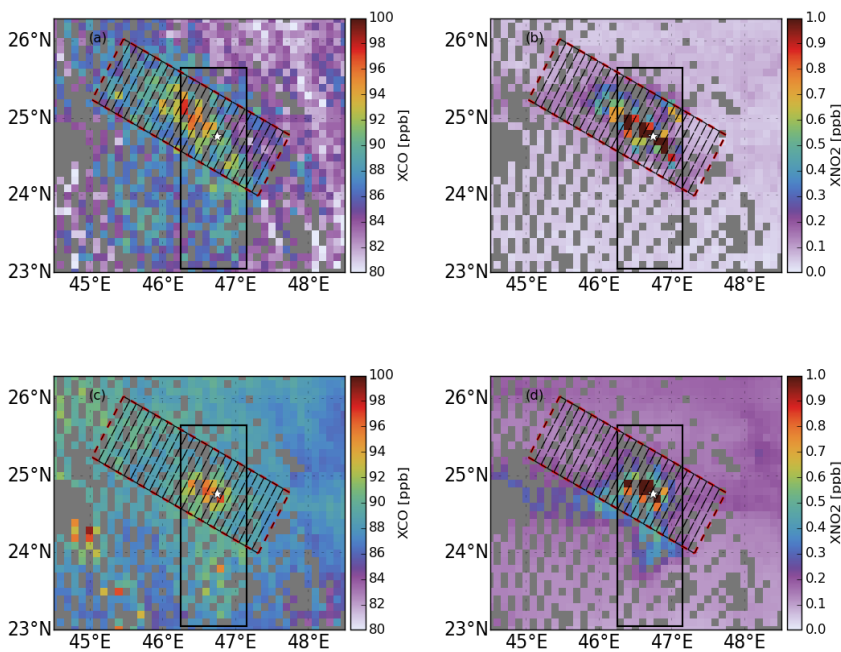
Figure S10. TROPOMI derived a) XCO, b) XNO_2 and WRF derived c) XCO and d) XNO_2 over Riyadh for 4th August, 2018. The white star represents the centre of Riyadh. The black box (B1) with a dimension of 300kmx100km is rotated depending upon the average wind direction 50 km radius from the centre of Riyadh at the TROPOMI overpass time resulting red box. For the calculation of zonally averaged NO_2 and CO, red box is divided into 29 smaller cells with the width (dx) ~11km. TROPOMI and WRF derived XCO and XNO_2 is gridded at 0.1°x0.1°.
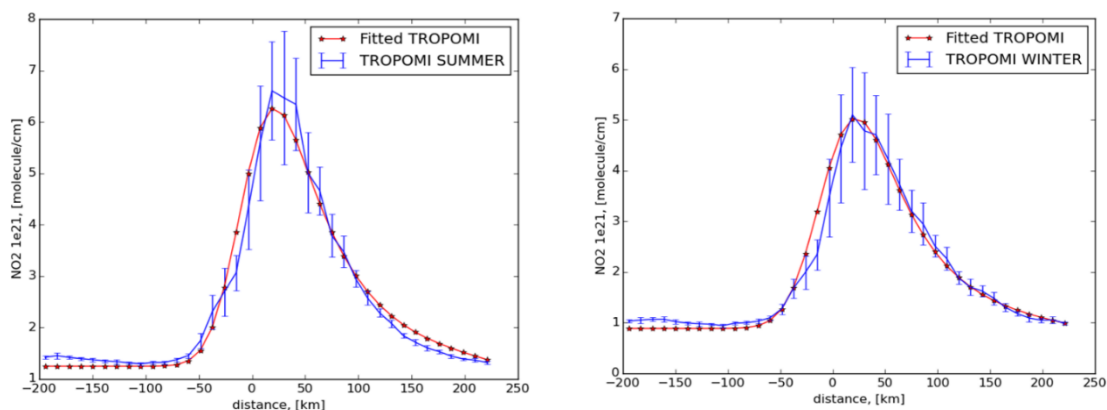
Figure S11. Zonally averaged NO2 tropospheric column densities (mean ±SME) for North east wind as a function of the distance over Riyadh (420 kmx250 km) for summer (left) and winter (right). The red line represents the fitted NO$_2$ column densities using EMG method. The correlation between observation and fit for summer is r^2= 0.94 and for winter is r^2= 0.96.
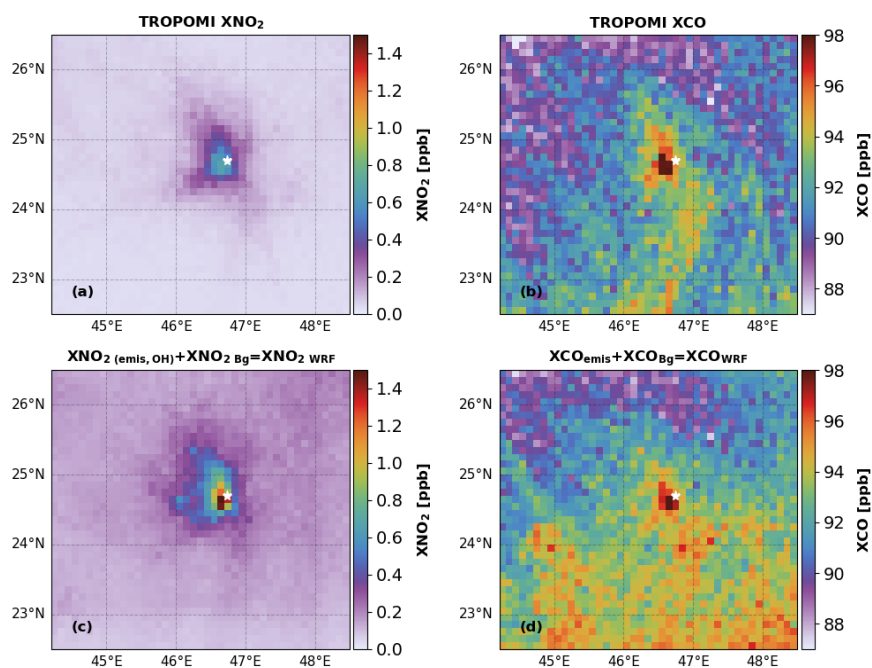
Figure S12. Co-located TROPOMI derived a) XNO$_2$ and b) XCO for November, 2018 to March, 2019 over Riyadh. Temporally, bilinear and vertically interpolated WRF simulated c)XNO$_2$ $_{WRF}$ and d) XCO $_{WRF}$ at the resolution of TROPOMI. The white star represents the centre of city. TROPOMI and WRF results are gridded at 0.1˚x0.1˚
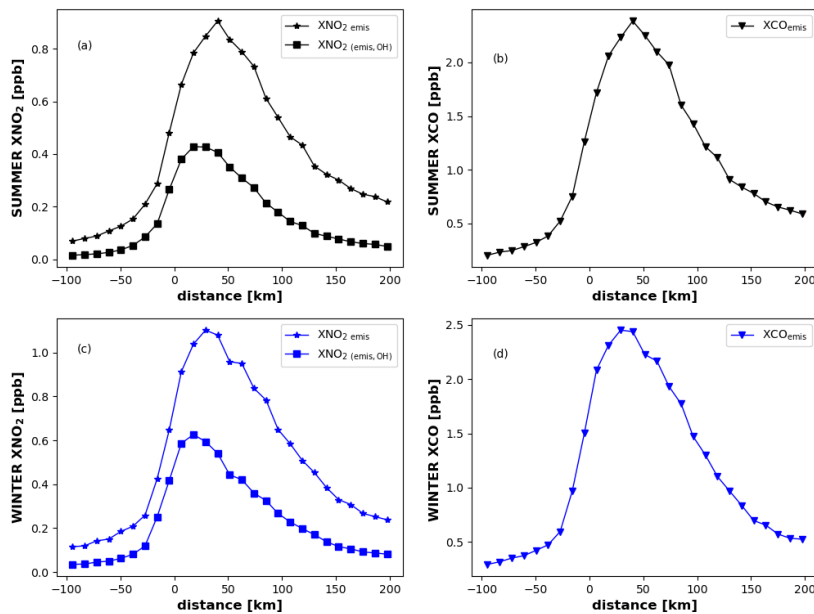
Figure S13. Zonally averaged a) summer $XNO_{2\,emis}$ and $XNO_{2\,(emis,\,OH)}$, b) summer XCO_{emis}, c) winter $XNO_{2\,emis}$ and $XNO_{2\,(emis,\,OH)}$ and d) winter XCO_{emis}. For the function of each of the tracer see Table 1.
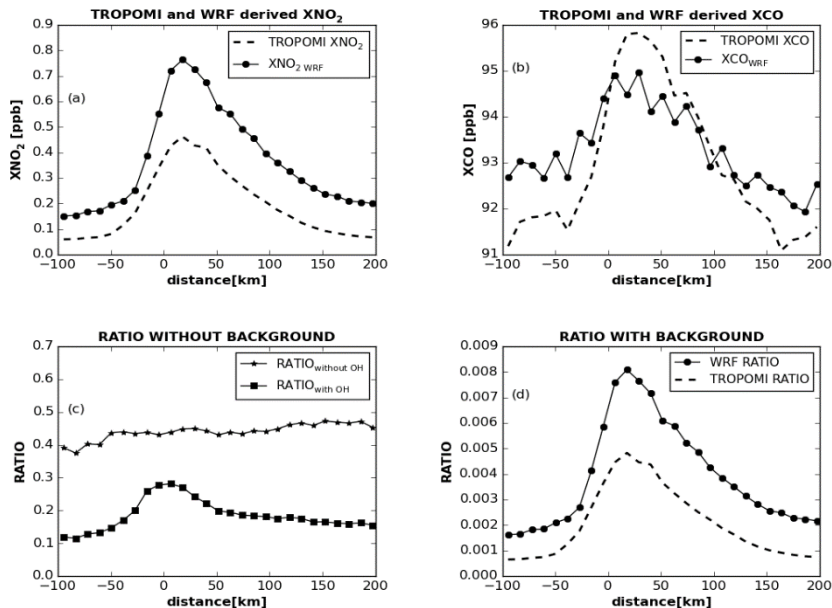
Figure S14. Comparison of WRF and TROPOMI zonally averaged a) XNO_2, b) XCO and c) WRF Ratio (XNO_2/ XCO) without CAMS background d) TROPOMI and WRF Ratio (XNO_2/ XCO) with background as a function of distance to the centre of Riyadh for winter (November, 2018 to March, 2019).
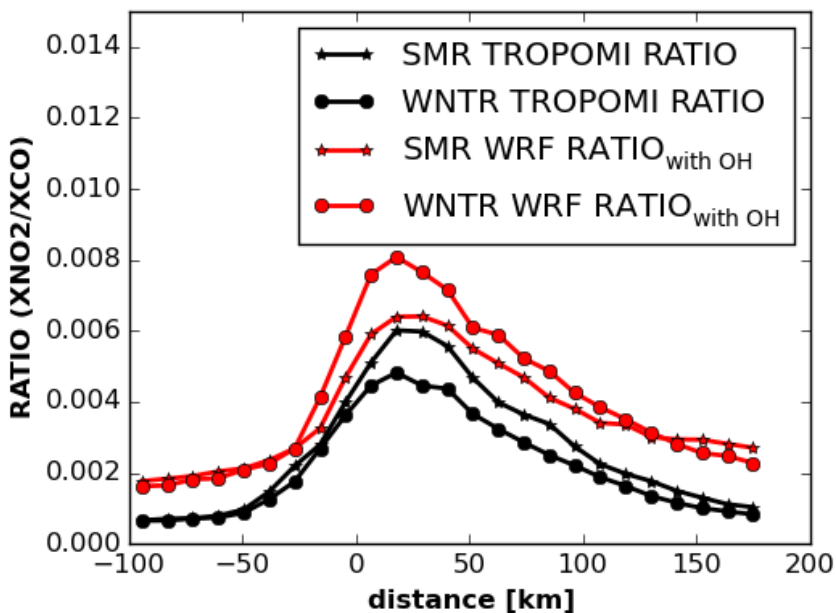
Figure S15. Comparison of WRF and TROPOMI derived Ratio (XNO_2/ XCO) as a function of distance to the centre of Riyadh for summer and winter.
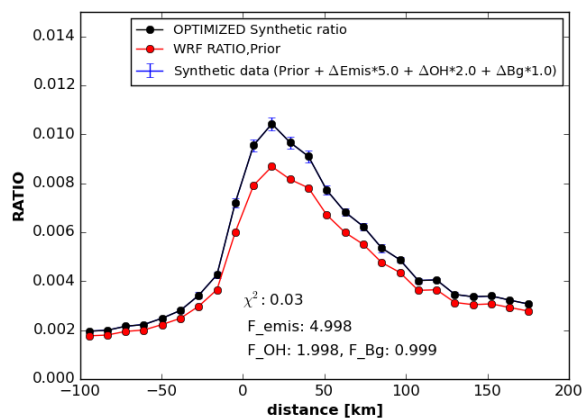
Figure S16. Summer (June to October,2018) averaged WRF derived Ratio before and after optimization in comparison to synthetic data (data ±std). F_{emis}, F_{OH} and F_{Bg} represents the scaling factor for emission, OH and background by which synthetic data is higher compared to WRF ratio.
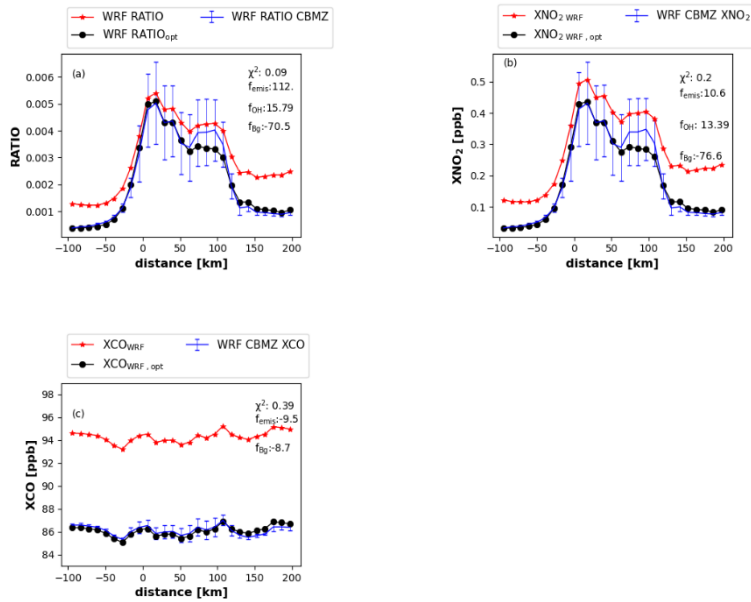
Figure S17. WRF derived a) XNO_2/XCO, b) XNO_2 and c) XCO before and after optimization in comparison to WRF using full chemistry with CBMZ chemical scheme for 17th August, 2018. f_{OH}, f_{emis} and f_{Bg} are optimized scaling factors obtained iteratively for OH, emissions and background by least square optimization method. f_{emis}, f_{OH} and f_{Bg} are derived by accounting the total change in emission, OH and background using the corresponding scaling factors obtained from 1st and 2nd iterative step. The unit of scaling factor is in percent (%).
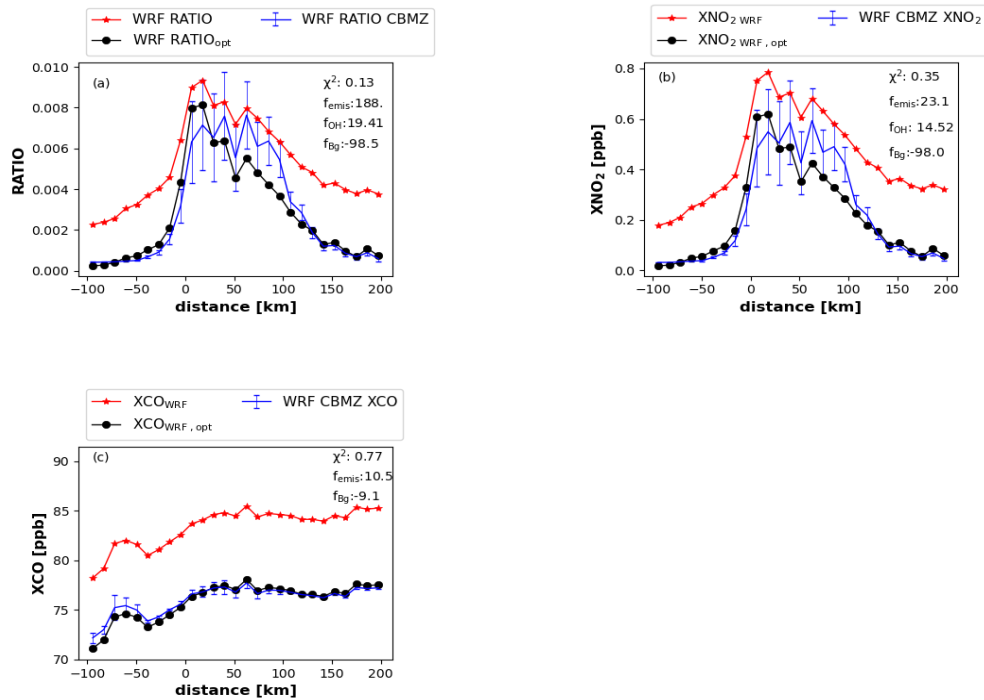
Figure S18. Same as Figure S17 but for 18th November, 2018.
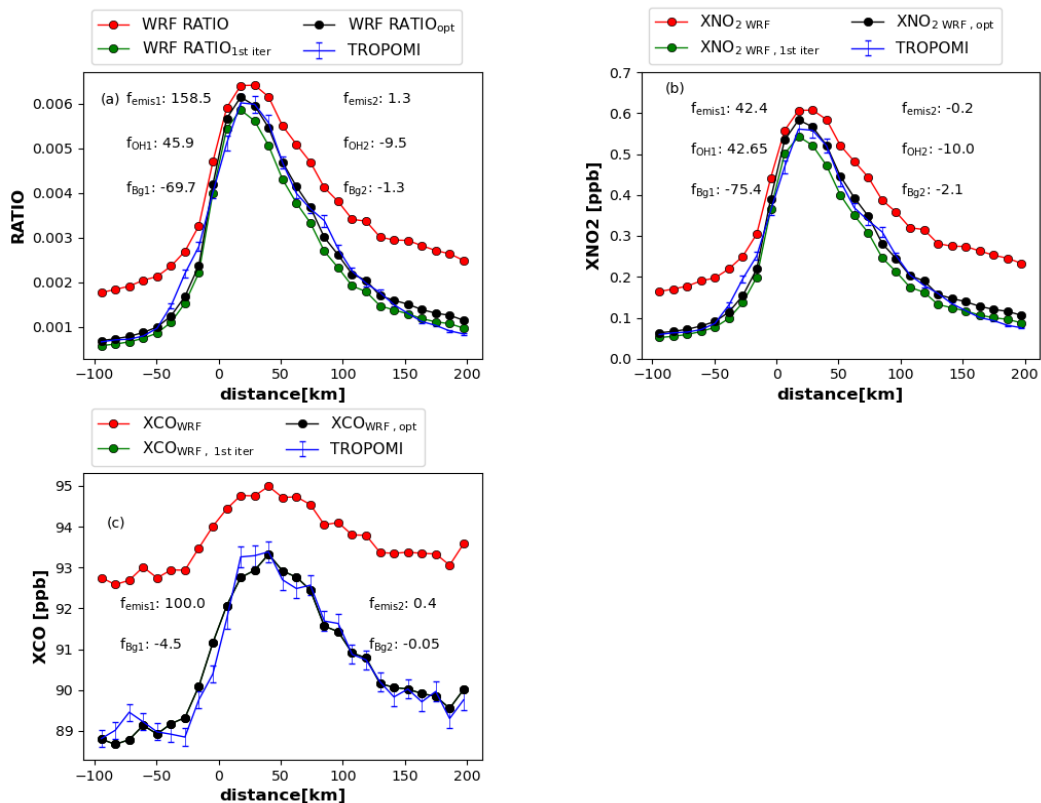
Figure S19. Summer (June, 2018 to October ,2018) averaged WRF derived a) Ratio, b) XNO_2 and c) XCO in comparison to TROPOMI. Step1: f_{OH1}, f_{emis1} and f_{Bg1} is the first scaling factor for OH, emission and background derived from least square method while comparing WRF prior run to TROPOMI. Step2: Change the emission , background and OH used in prior run by applying f_{OH1}, f_{emis1} and f_{Bg1} and derive **WRF Ratio $_{1st\ iter}$, $XNO_{2\ 1st\ iter}$** and **XCO $_{WRF,\ 1st\ iter}$**. Step 3: f_{OH2}, f_{emis2} and f_{Bg2} second scaling factor derived from least square method while comparing the result of 1st iteration to TROPOMI. Step 4: Apply f_{OH2}, f_{emis2} and f_{Bg2} to the emission, background and OH concentration used for 1st iteration and derive **WRF Ratio$_{opt}$, $XNO_{2\ WRF,opt}$** . To get the final scaling factor, divide the results of 2nd iteration by Prior run.
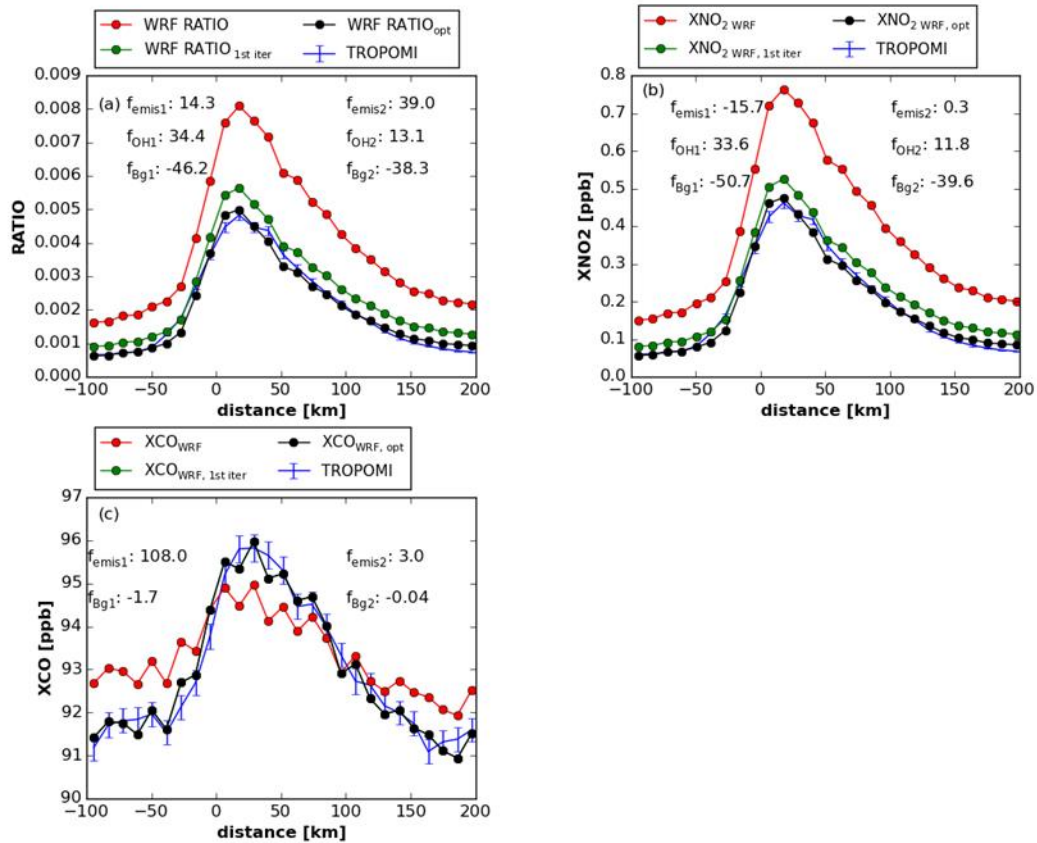
15

Figure S20. Same as Figure S10 but for Winter (November, 2018 to March,2019).
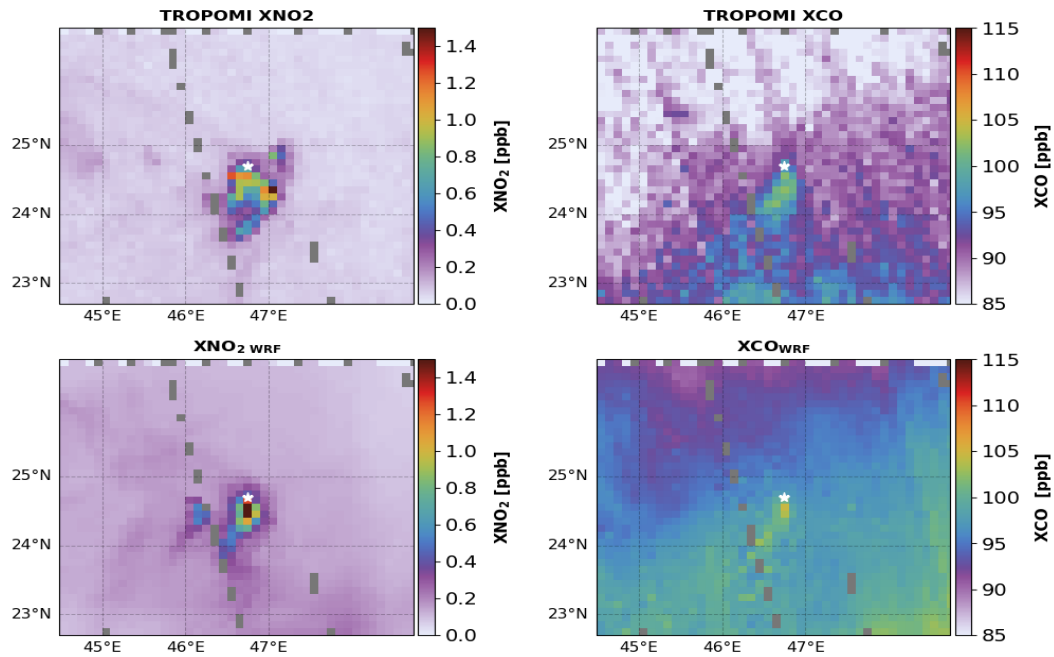
Figure S21. Comparison between XNO$_2$ (left) and XCO (right) from TROPOMI and WRF over Riyadh for 18th August , 2018 . Top panels show TROPOMI data and bottom panels the corresponding co-located WRF results. **XNO$_{2\text{ WRF}}$** is derived by adding **XNO$_{2\text{ (emis,OH)}}$** and **XNO$_{2\text{ Bg}}$** . **XCO$_{\text{WRF}}$** is derived by adding **XCO$_{\text{emis}}$** and **XCO$_{\text{Bg}}$**. The white star represents the centre of city. TROPOMI and WRF results are gridded at 0.1˚x0.1˚.
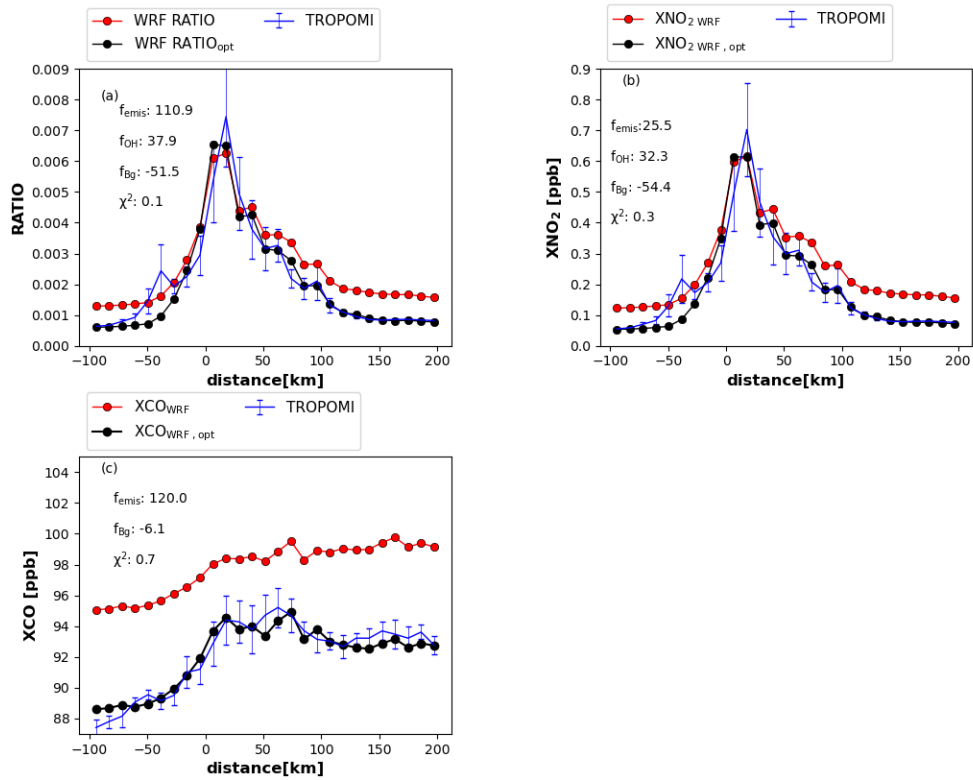
Figure S22. Comparison between TROPOMI and WRF, before and after optimization for 18th August, 2018. a) XNO_2/XCO ratio, b) XNO_2 and c) XCO in comparison to TROPOMI. f_{OH}, f_{emis} and f_{Bg} are optimized scaling factors obtained iteratively for OH, emissions and background by least square optimization method. f_{emis}, f_{OH} and f_{Bg} are derived by accounting the total change in emission, OH and background using the corresponding scaling factors obtained from 1st and 2nd iterative step. The unit of scaling factor is in percent (%).
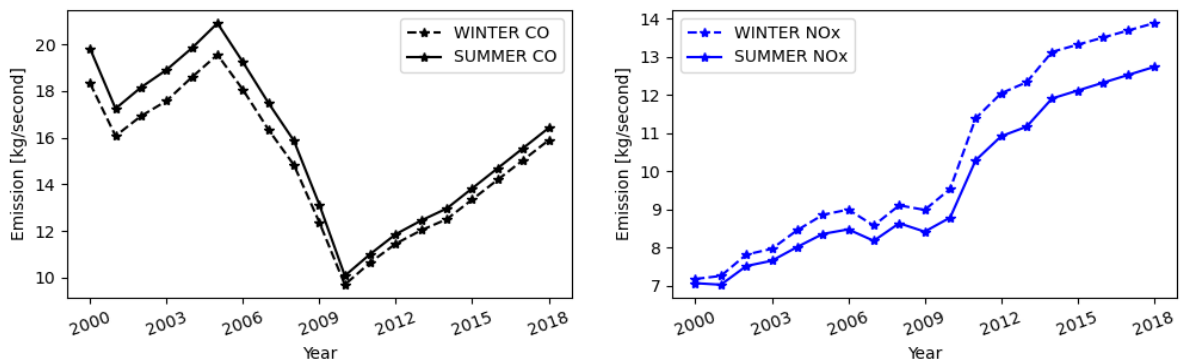

Figure S23. EDGAR a) CO and b) NOx emission from 2000 to 2018 for summer and winter at the time TROPOMI overpasses over Riyadh. EDGAR 2000 to 2015 data is linearly extrapolated to derived emission data for 2018.
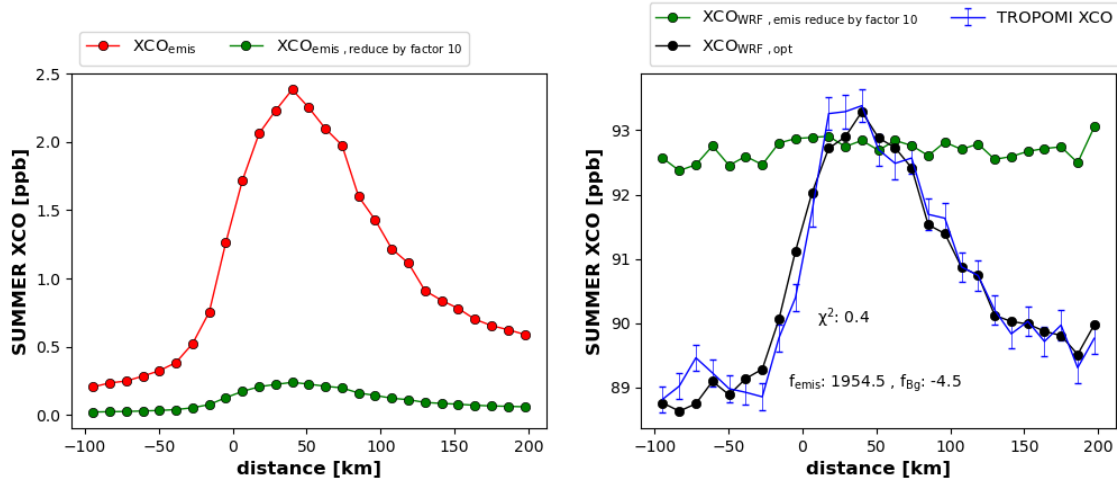
Figure S24. WRF derived XCO_{emis} before and after reduction by factor 10 (left). The comparison of TROPOMI derived XCO and $XCO_{WRF, emis\ reduce\ by\ factor\ 10}$ ($XCO_{emis,reduce\ by\ factor\ 10}$ + XCO_{Bg}) before and after optimization (right). The f_{emis} and f_{bg} are the scaling factor for emission and background. The unit is in percentage.
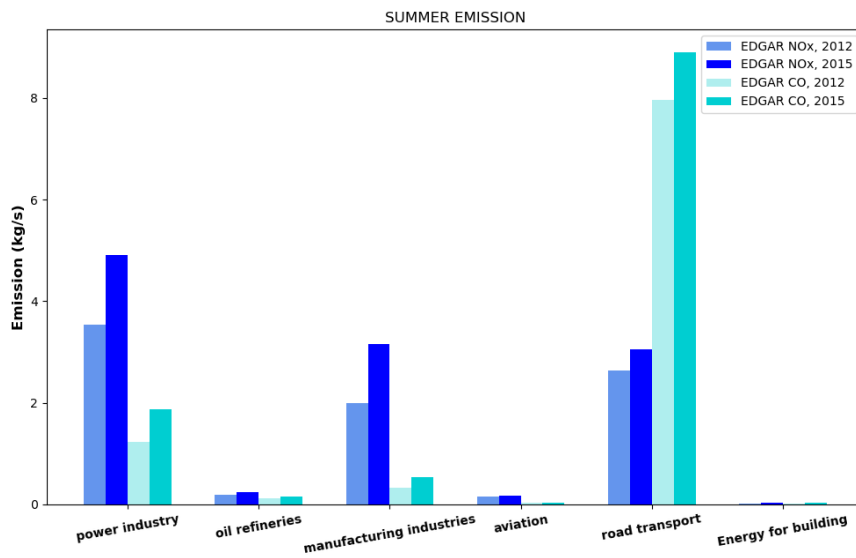

Figure S25. EDGAR NOx and CO emission for different source sectors for summer 2012 and 2015 at the time TROPOMI overpasses over Riyadh.
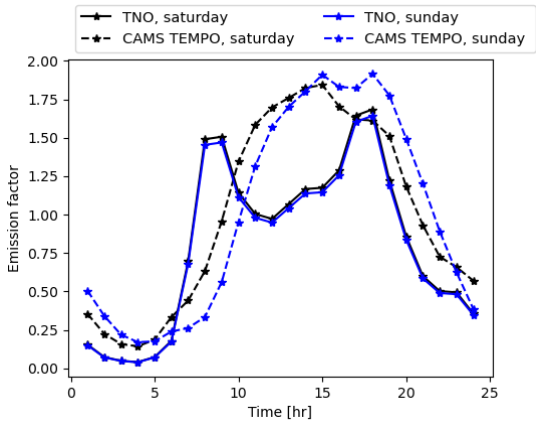
Figure S26 TNO Vs CAMS TEMPO emission for road transport during Saturday and Sunday**.**
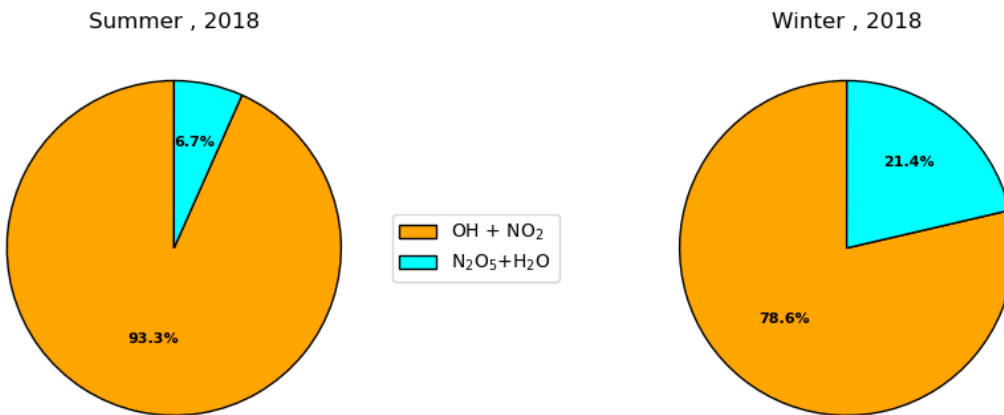

Figure S27. The different pathways of NOx loss over Riyadh at the time TROPOMI overpasses during summer (left) and winter (right) , 2018.